canceled by the resonant response of the coated cylinder. Otherwise, the energy can diverge (*4*, *5*). Because a single polarizable line dipole produces no induced moment, it follows that a collection of such objects would also produce no moment, and hence be invisible.

To realize all these possibilities requires ingenious materials design supported by advances in technology. There is a plethora of reported advances in both wave-functional materials fabrication, as well as the realization of related phenomena. Because many of the wave-functional effects are associated with resonances, overcoming the limitations imposed by dissipation and dispersion effects (meaning that the desired phenomena are realizable only within a narrow frequency window) represents the most urgent challenge. In this respect, the successful achievement of a photonic crystal optical cavity Q value on the order of 10^6 by Noda's group in Kyoto University (*6*) is noteworthy for foreshadowing the potential applications. There are also efforts to realize a negative refraction index through structural means, such as extreme anisotropy (*7*) and chiral materials (*8*), in addition to photonic crystals. An interesting proposal is to compensate the resonance-induced dissipation with an optical gain medium (*9*), which can be pumped separately. The degree to which these efforts are successful would set the scenario of future wave technology.

Wave localization in the Anderson sense (that is, localization of waves as they scatter in a random medium) is generally characterized spatially by an exponentially decaying wave function. However, if one uses a pulse to probe a medium with localized states, then it can be shown theoretically that there are also characteristic time-domain signatures (*10*). Recent experiments by Storzer *et al*. (*11*) have shown that by measuring time-resolved photon transport through TiO_2 powder samples, one can detect clear deviation from the diffusive behavior that is expected from multiple scatterings (*12*). Moreover, it was reported during the meeting that the deviation can be explained by a time-dependent diffusion constant D that approaches a ~$1/t$ behavior. If $r^2 \sim Dt$, then heuristically $D \sim 1/t$ implies a saturation length—the localization length. The photon mobility edge, the optical analog to the electronic metal-insulator transition, may be within reach.

Random systems are usually characterized by probability functions. Thus, wave localization, a manifestation of multiple scattering of waves in random media, has been mostly studied by focusing on the mean behavior, just as diffusion is the mean behavior of a random walker. A shift away from this focus is represented by the study of the "connectivity" of localized wave functions in a single (finite) random configuration. In a one-dimensional layered system, a connected state consisting of multiple localized wave functions (*13*) with roughly the same energy and equally spaced across the sample is denoted a "necklace." Such necklaces would carry most of the wave flux through the sample, because they represent short circuits in an otherwise insulating sample. In two separate experiments, one in the microwave regime by Sebbah *et al*. (*14*), and one in the optical regime by Bertolotti *et al.* (*15*), these necklace states in a one-dimensional layered system were observed. The true significance of these states may lie in the three-dimensional mobility edge, where in analogy with percolation the connected localized states would play a role similar to that of the percolating backbone, which has density measure zero (because of its fractal geometry) but nevertheless carries all the flux.

As the title of the meeting "From Random to Periodic" implies, some convergence of the two developments may be inevitable, or even anticipated. Challenges remain, however, in identifying the nontrivial intersections, from which new physics and phenomena may emerge.

References

1. Optical Society of America Conference on Photonic Metamaterials: From Random to Periodic, Grand Bahama Island, The Bahamas, 5 to 8 June 2006.
2. U. Leonhardt, *Science*, **312**, 1777 (2006).
3. J. B. Pendry, D. Schurig, D. R. Smith, *Science* **312**, 1780 (2006).
4. G. W. Milton, N.-A. P. Nicorovici, *Proc. R. Soc. A* 10.1098/rspa.2006.1715 (2006).
5. G. W. Milton, N.-A. P. Nicorovici, R. C. McPhedran, V. A. Podolskiy, *Proc. R. Soc. A* **461**, 3999 (2005).
6. B.-S. Song, S. Noda, T. Asano, Y. Akahane, *Nat. Mat.* **4**, 207 (2005).
7. V. A. Podolskiy, E. E. Narimanov, *Phys. Rev. B* **71**, 201101(R) (2005).
8. Y. Svirko, N. Zheludev, *Appl. Phys. Lett.* **78**, 498 (2001).
9. T. Klar, A. V. Kildishev, V. M. Shalaev, JSTQE-IEEE (2006).
10. B. White, P. Sheng, Z. Q. Zhang, G. Papanicolaou, *Phys. Rev. Lett*. **59**, 1918 (1987).
11. M. Storzer, P. Gross, C. M. Aegeter, G. Maret, *Phys. Rev. Lett*. **96**, 063904 (2006).
12. P. Sheng, *Introduction to Wave Scattering, Localization, and Mesoscopic Phenomena* (Springer, Berlin, ed. 2, 2006), chap. 5.
13. J. B. Pendry, *J. Phys. C* **20**, 733 (1987).
14. P. Sebbah, B. Hu, J. M. Klosner, A. Z. Genack, *Phys. Rev. Lett.* **96**, 183902 (2006).
15. J. Bertolotti, S. Gottardo, D. S. Wiersma, M. Ghulinyan, L. Pavesi, *Phys. Rev. Lett.* **94**, 113903 (2005).

10.1126/science.1131711

PHYSICS

Entangled Solid-State Circuits

Irfan Siddiqi and John Clarke

Quantum tomography is used to determine the entangled state of two coupled superconducting qubits, a step forward for solid-state quantum computing.

A fundamental tenet of quantum mechanics is the idea that two spatially separated objects exhibit correlations in observable physical properties that cannot be explained by any classical theory. Troubling even Einstein, this "spooky action at a distance" (*1*)— known as entanglement—is fundamental to quantum information science and directly related to the enhanced computing power of a processor based on quantum bits (qubits). What is remarkable is that solid-state electrical circuits containing as many as 10^{11} atoms can be engineered to exhibit quantum behavior and are well described by the quantum formalism originally developed for individual atoms and photons. One can construct such qubits from thin films using conventional semiconductor fabrication techniques, making them attractive for eventually realizing a quantum computer with many qubits.

With these solid-state "atoms on a chip," one can prepare arbitrary superpositions of single-qubit states and manipulate them with microwave radiation to observe clear signatures of quantum coherence familiar in atomic physics and nuclear magnetic resonance (*2*–*5*). Coupling two or more qubits together results in entangled states with energy spectra that exhibit features such as avoided crossings (*6*) predicted by quantum mechanics. Verifying that two qubits are unambiguously entangled is, however, a delicate task and requires sophisticated benchmarks such as quantum state tomography (*7*). This method involves a series of measurements (analogous

I. Siddiqi is in the Department of Physics, University of California, Berkeley CA 94720–7300, USA. E-mail: irfan_siddiqi@berkeley.edu J. Clarke is in the Department of Physics, University of California, Berkeley, CA 94720–7300, USA, and the Materials Sciences Division, Lawrence-Berkeley National Laboratory, Berkeley, CA 94720, USA. E-mail: jclarke@berkeley.edu

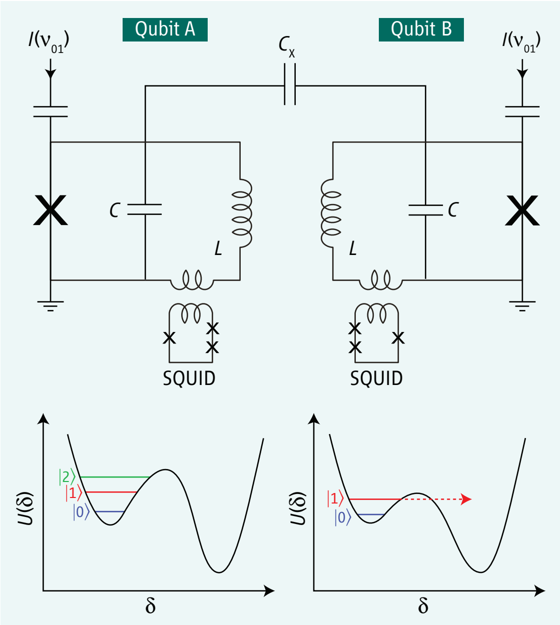

Coupled qubits. (**Top**) Simplified schematic of two phase qubits coupled by a capacitance and driven by microwave current sources $I(\nu_{01})$. (**Bottom left**) Potential-energy wells of a fictitious particle versus phase difference δ. The barrier height and level spacing are adjusted by an external magnetic flux. Microwaves induce transitions between the states $|0\rangle$ and $|1\rangle$ to create any chosen superposition. (**Bottom right**) Potential-energy wells with barrier height lowered by applying a fast flux pulse for qubit state measurement.

to the image "slices" that are captured and combined into a three-dimensional picture in tomographic medical imaging) to characterize the quantum state. In particular, such measurements are used to reconstruct the density matrix of the system, a mathematical tool that specifies the components of an arbitrary quantum state. On page 1423 of this issue, Steffen *et al*. (*8*) report an important advance in the first tomographic measurements of an entangled state produced by two coupled solid-state qubits.

Steffen *et al*. use two superconducting phase qubits, A and B, coupled by a capacitance C_x (see the figure, top panel). Each qubit consists of a Josephson tunnel junction (indicated by the X)—shunted with a capacitance *C*—in a superconducting loop of inductance *L*. The dynamics of the system are described by the motion of a fictitious particle representing the quantum variable δ, the difference between the phases of the superconducting order parameters on each side of the junction. This particle is confined to an asymmetric double-well potential $U(\delta)$ formed by applying an external magnetic flux (see the figure, bottom left panel). The two lowest energy levels in the shallow potential well on the left are the quantum states $|0\rangle$ and $|1\rangle$, separated by energy E_{01}. Fast microwave pulses at frequency $\nu_{01} = E_{01}/h$ (where *h* is the Planck constant) prepare any chosen superposition of $|0\rangle$ and $|1\rangle$ (transitions from $|1\rangle$ to $|2\rangle$ can be ignored because their energy difference is off-resonance). Once state preparation is complete, a fast flux pulse tilts the potential (see the figure, bottom right panel). If the qubit is in the state $|1\rangle$, the phase particle tunnels to the adjacent deep potential well, causing a sudden change in δ and inducing a magnetic flux that is stored in the loop. If the qubit is initially in the state $|0\rangle$, however, no tunneling occurs. The difference between these two flux states is readily detected with an on-chip SQUID (superconducting quantum interference device) inductively coupled to the qubit.

In the case of two coupled phase qubits, there are four basis states: $|00\rangle$, $|01\rangle$, $|10\rangle$, and $|11\rangle$ (where 0 and 1 indicate the state of each individual qubit). Steffen *et al*. prepare the entangled state $(|01\rangle - i|10\rangle)/\sqrt{2}$ (where $i = \sqrt{-1}$), one of the states that is important in quantum logic. The density operator for this state is $\hat{\rho} = (|01\rangle - i|10\rangle)(\langle 01| + i\langle 10|)/2$. The corresponding density matrix is

$$\rho = \begin{array}{c} \\ \langle 00| \\ \langle 01| \\ \langle 10| \\ \langle 11| \end{array} \begin{array}{c} \begin{array}{cccc} |00\rangle & |01\rangle & |10\rangle & |11\rangle \end{array} \\ \begin{pmatrix} 0 & 0 & 0 & 0 \\ 0 & 1/2 & -i/2 & 0 \\ 0 & i/2 & 1/2 & 0 \\ 0 & 0 & 0 & 0 \end{pmatrix} \end{array} \qquad (1)$$

Entanglement is indicated by the nonzero, off-diagonal elements of the density matrix, $i/2$ and $-i/2$; these particular off-diagonal matrix elements must be nonzero to represent an entangled state. If one instead had a product state of the form, $(|10\rangle + |00\rangle)/\sqrt{2} = (|1\rangle + |0\rangle)|0\rangle/\sqrt{2}$, there would be no quantum correlations between measurements of the states of the two qubits. Simply measuring qubit A, for example, cannot distinguish between the entangled and product states described above, and each measurement would yield a 50% probability of being in $|0\rangle$ or $|1\rangle$. A more sophisticated sequence, namely, state tomography, is needed to determine all the elements of the density matrix.

Arguably, George Stokes (*9*) introduced such a procedure in 1852 in the context of linear optics. Using a set of four measurements involving polarizers of various orientations, he reconstructed the polarization state of an unknown electromagnetic wave. In the case of coupled phase qubits, a tomographic measurement involves applying different microwave pulse sequences (similar to those in nuclear magnetic resonance) before readout to obtain different linear combinations of the elements of the density matrix (*10*). From this information, Steffen *et al*. reconstruct the density matrix. Their results convincingly show the signatures of their entangled state, namely, the diagonal and nonzero off-diagonal matrix elements shown in Eq. 1. After correction for known measurement errors, the observed magnitudes are 87% of the theoretical values. The remaining discrepancy is consistent with predictions based on the measured decoherence time.

These tomographic measurements are a positive step forward for solid-state quantum computing, representing a proof-of-principle demonstration of the basic functions needed for a quantum computer. At the same time, we are reminded of the complexities of the solid state, which has many possible channels of decoherence. Fidelity—control and measurement precision—may be lost to uncontrolled degrees of freedom that might be associated with the readout circuit, low-frequency noise in charge, flux, and junction critical current, and lossy circuit materials. Steffen *et al*. suggest that their observed loss of fidelity is a result of poor dielectric materials. Decoherence in other kinds of superconducting qubits is reduced by operating them at symmetry points at which they are insensitive to environmental noise (*3*), thereby implementing a level of hardware fault tolerance. Moreover, quantum error correction codes have been developed for software fault tolerance. Given the tremendous progress made with superconducting qubits in the past few years, we expect the demonstration of even more sophisticated quantum algorithms in the not-too-distant future.

References

1. A. Einstein, B. Podolsky, N. Rosen, *Phys. Rev.* **47**, 777 (1935).
2. Y. Nakamura, Yu. Pashkin, J. S. Tsai, *Nature* **398**, 786 (1999).
3. D. Vion *et al*., *Science* **296**, 886 (2002).
4. I. Chiorescu *et al*., *Science* **299**, 1869 (2003).
5. J. R. Petta *et al*., *Science* **309**, 2180 (2005).
6. J. Von Neumann, E. Wigner, *Z. Phys.* **30**, 467 (1929).
7. U. Leonhardt, *Phys. Rev. Lett.* **74**, 4101 (1995).
8. M. Steffen *et al*., *Science* **313**, 1423 (2006).
9. G. C. Stokes, *Trans. Camb. Philos. Soc.* **9**, 399 (1852).
10. I. L. Chuang *et al*., *Proc. R. Soc. London A* **454**, 447 (1998).

10.1126/science.1132544

Published by AAAS